SPECIMEN GEOMETRY EFFECTS ON 316L(N) CREEP CRACK GROWTH ANALYSES

Lucien Laiarinandrasana*, Moulay Rachid Kabiri[£]
*Centre des Matériaux P. M. Fourt, UMR CNRS 7633, Ecole des Mines de Paris
BP 87, F-91003 Evry Cedex France
[£]Département Matériaux et Procédés, Ecole Nationale Supérieure d'Arts et Métiers de Meknès
BP 4024, Béni M'hamed – Meknès Morocco
lucien.laiarinandrasana@ensmp.fr

Abstract

The ASTM E1457-98 standard [1] describes the procedure allowing to determine the master curve *da/dt* versus *C** parameter, for creeping solids. However, the methodology is only to be applied on CT specimens. The European collaborative program CRETE aims at extending the application of the ASTM E1457-98 standard to other types of laboratory specimens. In this paper, existing database of creep crack growth on 316L(N) stainless steel is utilised, concerning three types of specimens: Circumferentially Cracked Round Bars (CCRB) and Double Edge Notched Tensile specimens (DENT) for tensile mechanical loading whereas classical CT specimen combines tensile and bending loading modes.

The geometry effect is first investigated by introducing the *Q** parameter by analogy to *Q* parameter in the elastic-plastic *J-Q* approach. A modified procedure based on the ASTM E1457-98 standard has been applied to the database, allowing to plot a unique master curve *da/dt* vs *C**.

Introduction

In the ASTM E1457-98 standard [1], the procedure allowing to determine the master curve *da/dt* versus *C** parameter, for creeping solids is only recommended to be applied on (Compact Tension) CT type specimens. This geometry is known to favour bending effects in the remaining ligament. However, for actual engineering components working at high temperature, thermo-mechanical complex loading including either tensile or bending stress states may be encountered. The European collaborative programme CRETE aims at extending the application of ASTM E1457-98 standard to other types of laboratory specimens. In this paper, our contribution consists in gathering experimental data of creep crack growth on 316L(N) stainless steel, consisting of 14 tests on Circumferentially Cracked Round Bars (CCRB) and 2 tests on Double Edge Notched Tensile specimens (DENT) for tensile mechanical loading, and finally 10 tests on CT specimens combining tensile and bending loading modes.

The background concerning the discussion about the ASTM E1457-98 procedure has been published elsewhere by Laiarinandrasana *et al*. [2] and Kabiri *et al.* [3]. The main conclusions can be summarized as follows: i) the ASTM E1457-98 methodology allowing to separate the creep part of the load line displacement rate from the structural part (due to the crack advance) is recommended, provided that the stress state in the ligament is well known (plane stress PS or plane strain PE); ii) the lower limit of exploitable experimental creep

crack growth data is characterized by the point corresponding to the minimum load line displacement rate (avoiding tail effects); iii) the upper limit is based on the deviation from secondary (stationary) creep of the reference creep strain rate.

The first part of the paper investigates further the additive split of load line displacement rate. Finite Element (FE) results will be compared to the ASTM E1457-98 creep part. Then a $Q*$ parameter is introduced in order to quantify the loss of constraint for the aforementioned geometries. The expected influence of $Q*$ values are discussed before plotting the master curve da/dt vs $C*$ produced by all creep crack growth tests.

Analysis of the creep notch opening displacement rate

Displacement partitioning

The history of the opening displacement is provided in the database for each test. The total displacement δ_t is assumed to be the sum of the elastic δ_e, plastic δ_p and creep δ_c components. Assuming (i) that the structural part: $\delta_s = \delta_e + \delta_p$ is only due to the crack advance, so that the remainder (i.e. time dependent term) is due to the creep behaviour and, (ii), that there is no interaction between these two terms, the displacement rates can be written as follows:

$$\dot{\delta}_t = \dot{\delta}_e + \dot{\delta}_p + \dot{\delta}_c \qquad\qquad \dot{\delta}_t = \dot{\delta}_s + \dot{\delta}_c \qquad\qquad (1)$$

In the ASTM E1457-98 it is recommended that the rate contribution due to creep component $\dot{\delta}_c$ is deduced by subtracting the elastic-plastic from the total opening displacement rate, so that:

$$\dot{\delta}_c = \dot{\delta}_t - \dot{a}\frac{B}{P}\left[\frac{2K^2}{E} + (n_{pl} + 1)J_{pl}\right] \qquad\qquad (2)$$

where B is the thickness; P, the applied load; $\dot{a}$, the crack growth rate; E, the Young's modulus; K is the stress intensity factor, n_{pl} is the hardening exponent and J_{pl} is the plastic part of the Rice J-integral.

The $\dot{\delta}_c$ creep component is the relevant parameter allowing to calculate $C*$. The analytical expressions for respectively CT [1], DENT and CCRB specimens (Kabiri [4]) are given below:

$$C*(CT) = \left(2 + 0.522\left(1 - \frac{a}{W}\right)\right)\frac{n_2}{n_2 + 1}\frac{P\dot{\delta}_c}{B(W - a)} \qquad\qquad (3)$$

$$C*(DENT) = \frac{1}{2}\frac{n_2 - 1}{n_2 + 1}\frac{P\dot{\delta}_c}{B(W - a)} \qquad\qquad (4)$$

$$C*(CCRB) = \frac{n_2 - 1}{n_2 + 1}\frac{P\dot{\delta}_c}{2\pi R^2} \qquad\qquad (5)$$

where n_2 is the creep stress exponent, W the length of the remaining ligament and R the minimum radius of CCRB specimens. In the following, an attempt is made to compare FE results with equation (2).

Finite element calculation

FE computations with release node technique have been carried out by Kabiri [4] on 9 specimens (CCRB (5), DENT (1), CT (3)) in order to simulate the crack growth process. In order to describe the approach, we will focus on a CCRB specimen (denoted as CCRB1), tested at 600°C with *P=52630N*. The characteristic dimensions are: nominal diameter $\Phi =$ *11.5mm*, initial crack depth ratio $a_0/\Phi=0.45$ $(R = \Phi - a_0)$. The crack incubation time is *25h* and the crack growth is illustrated in Fig.1.
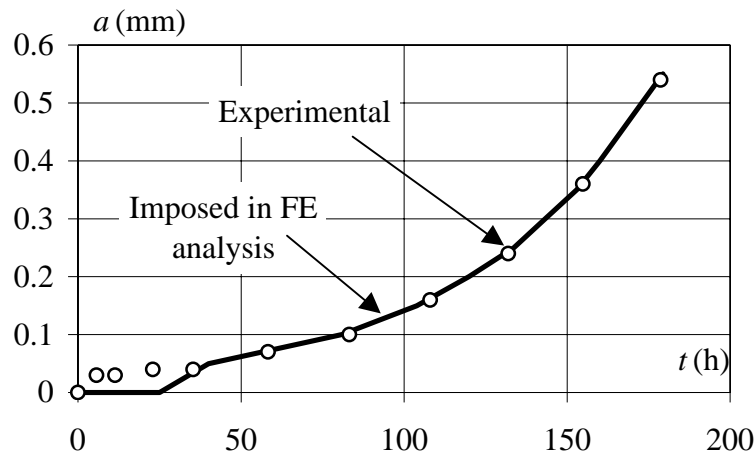

FIGURE 1: Crack growth curves for CCRB1 specimen

The FE computation uses 2D axi-symmetric iso-parametric elements with reduced integration. Only half of the geometry is meshed. The load is applied to the node set at the top of the mesh whereas the crack growth is numerically imposed by gradually releasing the nodes (12 steps) in the remaining ligament following *a(t)* in Fig.1. The constitutive equations are based on double inelastic deformation (DID) approach (Cailletaud and Saï [5]), allowing to separate the plastic and visco-plastic strains. The total opening displacement history simulation is reported in Fig.2, labelled as "propagating crack". It has been verified [4] that there is good agreement between experimental and FE simulation on propagating crack.

Then, extracting the creep component of the opening displacement consists in running several finite FE analyses of the same specimen but with various constant crack depth ratios. For a fixed value of a/Φ, ranging from a_0/Φ to $(a_0+550\mu m)/\Phi$, simulations are performed up to the time when the propagating crack reaches the actual a/Φ. In Fig.2, let us select the dashed line corresponding to the simulation of a stationary crack at $a = a_0+300\mu m$. This crack advance of *300μm* is reached at time $t = 143.3h$. The total amount of the opening displacement is *231μm*. The simulation of stationary crack corresponding to $(a_0+300\mu m)$ is performed up to $t = 143.3h$. Then, δ_c is supposed to be the numerical value of the opening displacement at that time: $\delta_c = 185\mu m$. The remainder is identified as the structural component due to the crack advance: $\delta_s = 46\mu m$. Conversely to the ASTM procedure, this methodology enables to directly estimate δ_c.

Before going further, some aspects about the lower and upper limits of validation of the experimental points obtained during the creep test have to be recalled. The lower limit is considered to be the point corresponding to the minimum opening displacement rate [2-3], allowing to avoid the tail effect due to the strain rate decrease (primary creep). The upper limit is generally reported to be determined by calculating the inelastic ratio: $\dot{\delta}_c / \dot{\delta}_t > 0.5$. Since $\dot{\delta}_c$ is supposed to be correctly evaluated, we suggest not to compare it with $\dot{\delta}_t$ but to check if $\dot{\delta}_c$ is still in the domain of secondary creep, in spite of crack propagation. To do this, the reference length l_{ref} concept is introduced (Piques [6]):

$$\delta = l_{ref}.\varepsilon_{ref} \qquad\qquad \sigma_{ref} = \sigma_0 \frac{P}{P_0} \tag{6}$$

P_0 is the limit load, generally given by handbooks (see e.g. [6]), σ_0 is the yield stress, ε_{ref} is the reference strain corresponding to the reference stress σ_{ref} in the uniaxial stress-strain curve. As long as secondary creep behaviour is involved and by analogy to plasticity:

$$\dot{\varepsilon}_{ref} = B_2 \sigma_{ref}^{n_2} \tag{7}$$

where B_2 and n_2 are material secondary creep coefficients. Additionally, [6]

$$l_{ref} = \gamma(W - a) \tag{8}$$

γ being a constant. Provided that the creep behaviour is in the secondary stage, equations (6-8) lead to:

$$\frac{\dot{\delta}_c}{(W - a)B_2 \sigma_{ref}^{n_2}} = \gamma \tag{9}$$

The upper limit is then defined as the deviation from equation (9), i.e. the ratio is no longer constant. Note that this condition allows an acceleration of the δ_c due to crack propagation (decrease in *(W-a)* results in increase in σ_{ref}).

For CCRB1 specimens, test results are such that $t_{lower} \cong 80h$ and $t_{upper} \cong 154h$.

From the curves plotted in Fig.2, the displacement rates are calculated. The results are illustrated in Fig.3 where we have focused the plot on the validation time range *80h < t < 154h*. Open symbols refer to results deduced from FE analysis whereas full symbols correspond to exploitation of the experimental data. So, starting form "total experimental" curve (full squares), the elastic-plastic contribution is calculated following ASTM recommendation, leading to the curve labelled "Structure ASTM" (full circles). The required creep component of displacement rate is deduced *via* equation 2, giving the curve labelled "Creep ASTM" (full triangles).

For the simulated quantities, "Total FE" (open squares) is the initial curve, then "Creep FE" (open triangles) is obtained by using the aforementioned procedure (see Fig.2) and "Structure FE" (open circles) stands for the structural term due to the crack advance by subtraction of "Creep FE" from "Total FE".

Fig.3 clearly shows that there is excellent agreement between "Creep ASTM" and "Creep FE". The same trends have been observed for all simulated tests although for DENT and CT specimens the stress state hypotheses (PE or PS) induce a larger scatter.
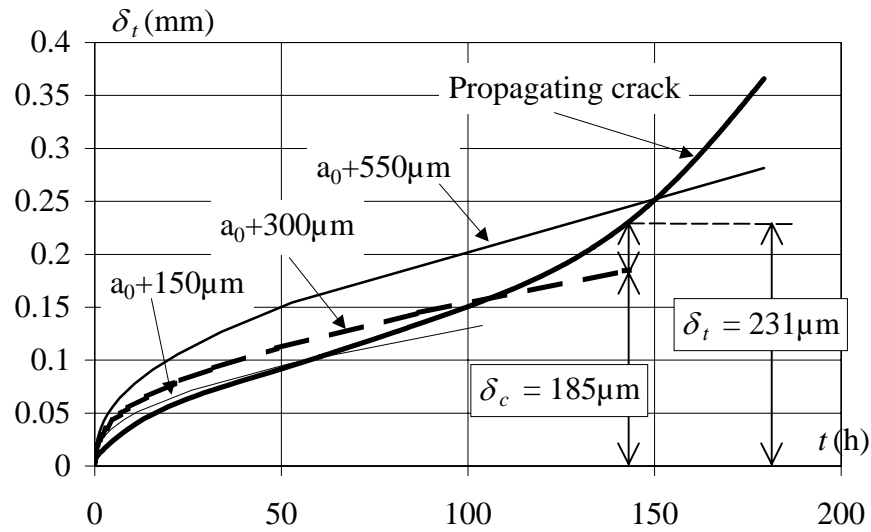

FIGURE 2: Determination of δ_c

Some comments should be added concerning C^* calculations. The numerical integration of the C^* parameter utilizes the creep strain rate (hence creep displacement rate). It has been reported [4] that the values of C^* given by numerical calculations and by equations (3-5), respectively, are in good agreement. Additionally, by using creep displacement rate value given by ASTM in equations (3-5), C^* values are found to be similar. In conclusion, numerical C^* values calculated for a propagating crack coincide well with the ASTM method based on the displacement rate partitioning.
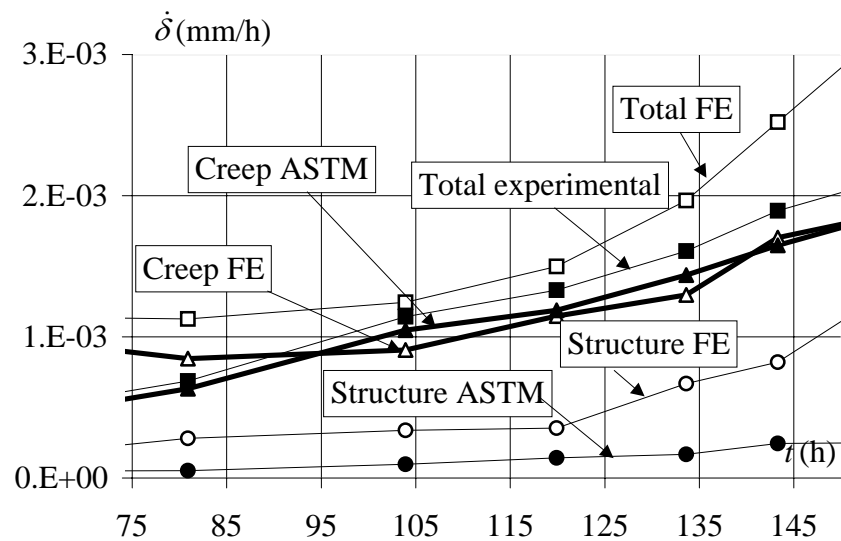

FIGURE 3: displacement rate partitioning, CCRB1

Plane stress – plane strain conditions

We mentioned that PS or PE conditions may increase the scatter in the C* calculations. These assumptions interfere in the elastic-plastic components in order to estimate the ASTM structural displacement rate for CT and DENT specimens. CCRB specimens do not require any assumption but this geometry is not mentioned in any current standard, hence there is no formula allowing to calculate the J_{pl} value with the EPRI method (Kumar et al. [7]).

Comparison between experimental and simulated elastic-plastic initial loadings indicates that CT specimens are globally close to PE conditions, whereas DENT specimens are close to PS conditions. CCRB will be supposed to follow the same trend as the DENT specimens under PE conditions. It has to be mentioned that the stress state (PE, PS) is supposed to be maintained during the whole creep test. However, some experimental data seem to indicate (Laiarinandrasana [8]) that whereas during the pre-loading sequence (elastic-plastic conditions) the specimen is close to PE condition, when the creep strain increases, the comparison between experimental and simulated $\delta(t)$ shows an evolution of the stress state towards the PS condition even when the specimens are side grooved [7].

Q* estimates

Following the J-Q approach in plasticity, a Q* parameter is introduced in order to evaluate the loss of constraint in the vicinity of the crack tip.

$$Q* = \frac{\sigma_{22}^{FE} - \sigma_{22}^{RR}}{\sigma_0} \tag{10}$$

where $\sigma_{22}^{FE}, \sigma_{22}^{RR}$ are respectively the numerical opening stress, the analytical opening stress according to the Riedel and Rice (RR) [9] stress field, the yield stress. In plasticity, it is recommended to capture the Q value at a distance r satisfying $2 < r/(J/\sigma_0) < 5$. In visco-plasticity the time singularity induces both stress relaxation and a progressive shift of the location of the maximum of the opening stress. Caution has to be paid when determining the Q* stabilization distance. Note also that the initial value of Q* is Q.

By assuming that the limit load is appropriate for the comparison, its value changes either for the same specimen with various a/W ratios, or from one specimen geometry to another. Works are still going on following Neimitz et al. [10] by comparing Q* value with respect to increasing J-integral.

The main conclusions of the Q* calculations are summarized as follows: for DENT under PS condition, $Q \cong Q* \cong 0$ whereas for both CT and DENT under PE condition, hence CCRB, $Q* < Q < 0$.

Significance of negative values of Q*

Equation 10 clearly indicates that Q* evaluates the difference between the opening stresses obtained by the FE method (including the non singular stress) and by analytical calculations (RR field) respectively. Accordingly, $Q* < 0$ means that the numerical value of the opening stress is less than the analytical one. Furthermore, the condition $Q* < Q < 0$ indicates that the numerical stress relaxation is greater than that of the RR-field.

Now, by considering that the maximum principal stress (opening stress) plays a major role on the creep damage evolution [6], assessments based on the RR field opening stress should lead to a pessimistic (conservative) prediction. Furthermore, as the RR stress field depends on the value of C*, the conclusion should be the same for C* based determination of da/dt or incubation time.
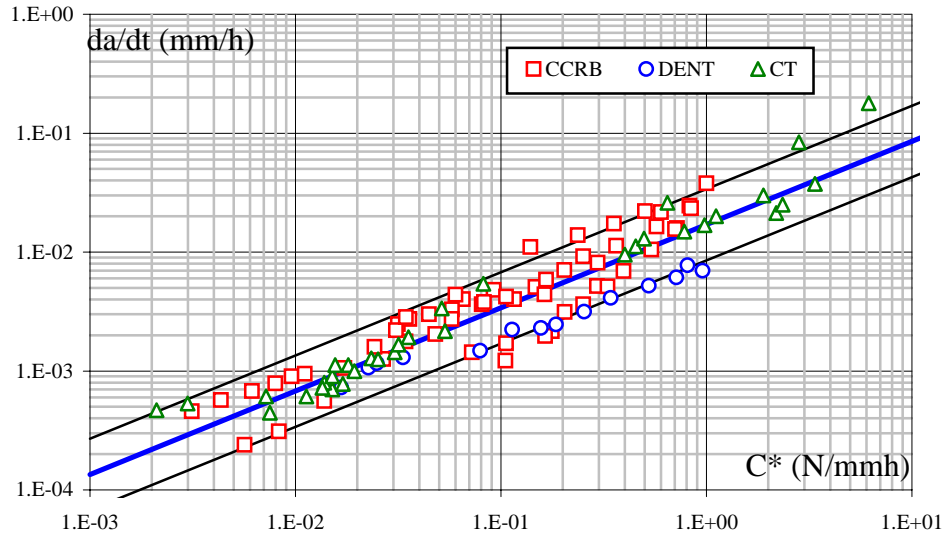
Master curve da/dt-C*

FIGURE 4: da/dt versus C* plot for CCRB, DENT and CT specimens.

In Fig.4, *C** values are calculated according to equations (3-5) but, as mentioned earlier, they are similar to numerical values of the *C** integral. Fig. 4 shows that paradoxically to the conclusion about the opening stresses, there is no influence of the specimen geometry on the master curve. From an engineering viewpoint this might be interesting in the sense that the same curve can be produced regardless the specimen geometry. However, it is desirable to analyse how large is the safety margin (conservatism) when using the master curve.

In ductile/brittle fracture approaches, it is known that bending specimens like CT induce conservatism on the crack growth or initiation prediction. According to O'Dowd et al [11], J_{1C} *(CT)* < J_{1C} *(DENT)* and regarding the *J-Δa* curves, the same value of the *J* load parameter leads to more propagation for CT specimen compared with DENT (Eisle et al. [12]). As tensile specimens (DENT, CCRB) results lay in the same scatter-band as CT specimens, Fig.4 shows that this conservatism is probably maintained.

Additionally, as the opening stress related to the *C** value is overestimated compared with the numerical one, we can guess that, at least for laboratory specimens for which the load is higher than or equal to the limit load, the master curve *da/dt* vs *C** prediction is likely to be conservative. This conservatism (safety margin) can be quantified by applying a local approach concept for which a creep damage parameter is introduced and connected to local variables such as the maximum principal stress, instead of a global parameter such as C*.

Conclusion

An experimental database on 316L(N) material consisting of 10 crack growth tests on CT specimens, 14 tests on CCRB specimens and 2 tests on DENT specimens has been selected

for extending the ASTM procedure to produce creep crack growth *da/dt* vs *C** master curve. The displacement rate partitioning suggested in the ASTM has been verified with FE analysis by using the node release technique. Hence, numerical *C** values computed on a propagating crack are in agreement with those obtained by simplified methods (e.g. EPRI). Furthermore, a second parameter *Q** (similar to *Q* in plasticity) has been introduced and calculated, resulting in *Q* < Q < 0*. Thus, the numerical opening stress -accounting for real boundary conditions- is lower than that of the RR stress field. Additionally, the master curve seems to be insensitive to the investigated specimen geometry. These results concerning laboratory tests (high load level) seem to indicate that a creep crack growth prediction *via da/dt* vs *C** curve should be conservative.

References

1.   ASTM E1457-98, *Standard Test Method for Measurement of Creep Crack Growth Rates in Metals*, 1998.

2.   Laiarinandrasana, L., *et al.* In *Proceedings of the 16th International Conference on Structural Mechanics in Reactor Technology*, edited by A. Gupta, Washington, U.S.A., 2001 (Cdrom).

3.   Kabiri, M.R., *et al.* In *Proceedings of the 17th International Conference on Structural Mechanics in Reactor Technology*, edited by S. Vejvoda, Prague, Czech Republic, 2003 (Cdrom).

4.   Kabiri, M.R., *High temperature cracking of steels : effects of geometry on creep crack growth laws*, PhD thesis Ecole Nationale Supérieure des Mines de Paris, 2003, *in French*

5.   Cailletaud, G. and Saï, K., *Int. J. of Plasticity*, vol.**11**, n°8, 991-1005, 1995.

6.   Piques, R., *Mechanics and mechanisms to crack initiation and growth under viscoplastic conditions in an austenitic stainless steel*, PhD Thesis, Ecole Nationale Supérieure des Mines de Paris, 1989, *in French*.

7.   Kumar, V., German, M.D., Shih, C.F., *An engineering approach for elastic-plastic fracture*, EPRI report NP 1931, 1981.

8.   Laiarinandrasana, L., *High temperature crack initiation in an austenitic stainless steel,* CEA, Report CEA-R-5692(E), 1996.

9.   Riedel, H. and Rice, J.R., *Tensile cracks in creeping solids*, Fracture Mechanics ASTM STP 700, 112-130, 1980.

10.   Neimitz, A., Dzioba, I., Galkiewicz, J., Molasy, R., *Engineering Fracture Mechanics*, vol. **71**, 1325-1355, 2004.

11.   O'Dowd, N.P., Shih, C.F., Dodds, R.H., In *Constraint Effects in Fracture : Theory and Applications*, vol.2, ASTM STP 1244, edited by M. Kirk, A. Bakker, 134-159, 1995.

12.   Eisle, U., Roos, E., Seidfuss, M., Silcher, H., *Determination of J-integral based crack resistance curves and initiation values for the assessment of crack large-scale specimens*, Fracture Mechanics, ASTM STP 1131, 37-59, 1992